UPPSALA
UNIVERSITET

Removal of heat-released DSB

Andris Abramenkovs

Degree project in biology, Bachelor of science, 2011
Examensarbete i biologi 15 hp till kandidatexamen, 2011
Biology Education Centre and Department of Biomedical Radiation Sciences , Uppsala University
Supervisor: Prof. Bo Stenerlöw

LIST OF ABBREVIATIONS

53BP1	p53-binding protein 1
ATM	Ataxia-Telangiectasia-Mutated
ATR	Ataxia-Telangiectasia and Rad3 Related
BER	Base excision repair
DNS	Deoxyribonucleic acid
DNA-PKcs	DNA-dependent protein kinase catalytic subunit
DSB	Double-strand break
EDTA	Ethylenediaminetetraacetic acid
EGFR	Endothelial growth factor receptor
FEN1	Flap specific-endonuclease 1
H2AX	Histone 2A variant X
HR	Homologous recombination
IR	Ionizing radiation
kbp	Kilobase pair
Mbp	Megabase pair
MMS	Methyl methanesulfonate
MRE11	Meiotic recombination 11
NHEJ	Non-homologous end joining
PARP-1	Poly(ADP-ribose) polymerase-1
P3KK	Phosphatidylinositol–3 kinase-related kinases
PFGE	Pulsed-field gel electrophoresis
SSA	Single-strand annealing
SSB	Single-strand break
XLF	XRCC4 like factor
XRCC	X-ray cross-complementary

CONTENTS

SUMMARY

It is known that chemical agents and ionizing radiation can induce alkali- and heat-labile sites in DNA. Two closely spaced heat-labile sites on opposite DNA strands or a heat-labile site opposite to a single-strand break could be transformed into a double-strand break after heating. One of the main techniques used for measurement of DSBs is pulsed – field gel electrophoresis (PFGE). For a long period of time the sample step in preparing naked DNA for PFGE involved heating. Therefore when PFGE was used in combination with heat-labile sites inducing agents, the obtained results for DSB measurement were misleading. An important question is if heat-labile sites can be transformed into DSB *in vivo* and thereby contribute to the toxic effects of ionizing radiation.

Non-homologous end joining (NHEJ) has been estimated to be the most active pathway that rejoins DSBs in mammalian cells. A consequence of introducing heat-labile sites in the measurements is that the kinetics of NHEJ appears to be faster and therefore higher NHEJ capacity of DSB rejoining is estimated.

The ability of methyl methanesulfonate (MMS) to alkylate DNA has been known for several decades. So far there is no evidence that MMS can cause true DSBs and therefore it was used to induce heat-labile sites. After treatment of MMS and elevated temperature DSBs are formed.

Therefore the aim of the study was to determine the impact of non-homologous end joining on heat-labile site removal induced by a chemical agent.

This study demonstrates that removal of heat-labile sites induced by MMS is relatively slow. There was no change in repair kinetic pattern when DNA-dependent protein kinase catalytic subunit (DNA-PKcs) was inhibited and a DNA-PKcs deficient cell line showed similar removal rate of MMS induced heat-labile sites as cells with wild type DNA-PKcs. Data from immunocytochemistry showed phosphorylation of DNA-PKcs that colocalized with p53-binding protein 1 (53BP1) foci. Lower amounts of DNA-PKcs activation and colocalization with 53BP1 was observed in X-ray cross-complementary 1 (XRCC1) deficient hamster cells.Therefore involvement of NHEJ in chemically induced heat-labile site removal is still unclear. This study also suggests that ionizing radiation induced heat-labile sites are different from heat-labile sites induced by MMS.

1.INTRODUCTION

1.1. Double-strand breaks

Damage of DNA in cells occurs due to environmental agents and endogenous processes. DNA double-strand breaks (DSBs) are thought to be one of the most cytotoxic forms of DNA damage (*Kass and Jasin, 2010; Falk et al. 2010*) and misrepair of DSBs can lead to carcinogenesis, genome instability, chromosomal rearrangement, mutations (*Kass and Jasin, 2010*) and cell death (*Falk et al. 2010*). Different mechanisms can contribute to formation of DSBs and it has been observed that DSB can be a result of single-strand breaks (SSBs) that are closely spaced and on opposite sides. Also DBSs can be produced if two oxidised bases or two apurinic/apyrimidinic bases are close to each other. DSBs can be induced when DNA polymerases δ or ε repairs one strand of DNA and encounters SSB on the opposite DNA strand (*Vispe and Satoh, 2000*).

1.2.Repair and signalling of double-strand breaks

1.2.1. Signalling of double-strand breaks

DSBs cause activation of complicated interactions between signalling proteins that sense DSBs. Signal transduction is conducted by members of Phosphatidylinositol – 3 kinase-related kinases (P3KK) family. Important role from PIKK family plays Ataxia-Telangiectasia-Mutated (ATM), Ataxia-Telangiectasia and Rad3 Related (ATR) and DNA-dependent protein kinases catalytic subunit (DNA-PKcs). It has been estimated that ATM and ATR are capable to interact with more than 700 proteins in response to DNA damage (*Bohgaki et al., 2010*). It has also been demonstrated that a member of the ErbB protein family, EGFR, is involved in regulation of non-homologous end joining (NHEJ) activity (*Kriegs et al. 2010*).

1.2.2. Homologous recombination and single-strand annealing

Eukaryotic cells are repairing DNA DSBs using three different pathways – homologous recombination (HR), single-strand annealing (SSA) and NHEJ (*Iliakis,*

2009; Rassool, 2003; Taleei et al., 2011). NHEJ is the most used mechanism in higher eukaryotes for DSB repair (*Wang et al., 2003; Taleei et al., 2011*).

Homologous recombination repair is a critical process for ensuring genomic stability in living organisms. This repair system is relatively precise and uses an existing homologous DNA segment as a template for damage repair (*Mazin et al., 2010; West, 2003*). For normal function of HR proteins such as RAD51, RAD52, RAD54, RPA, BRCA1, BRCA2 and others are required (*West, 2003*). HR repair is not functioning in the G1 phase of the cell cycle and achieves the highest efficiency in the S phase (*Mao et al., 2008; Frankenberg-Schwager et al., 2009*).

SSA repair process involves the same proteins as HR repair, but the mechanism of repair is completely different. During SSA two ends of DSB are joined together if the same sequence is found on both strands. This repair process is not sequence preserving because some of removed bases are not replaced and SSA can cause translocations (*Taleei et al., 2011*). It has been demonstrated that SSA is active during the S phase of the cell cycle (*Frankenberg-Schwager et al., 2009*).

1.2.3. Non-homologous end joining

NHEJ involves Ku70/Ku80, DNA ligase IV, XLF, XRCC4, MRN complex, DNA-PKcs, Artemis and DNA polymerases – polμ and polλ (*Hiom, 2010; Dobbs et al., 2010*). NHEJ is active during all cell cycle stages. The higher efficiency of NHEJ is in G2/M followed by S and G1 cell cycle phases (*Mao et al., 2008*). NHEJ does not ensure DNA sequence restoration (*Hiom, 2010)*.

The Ku protein is a heterodimer and consists of two subunits (Ku70 and Ku80) with relative molecular masses of 70 000 and 80 000 Da. This protein forms two rings that enclose DNA and has a high-affininty for DNA terminus. The dissociation constant has been estimated to be $1.5 - 4 \cdot 10^{-10}$M. It also has a region for interaction with DNA-PKcs (*Walker et al., 2001*). The Ku protein is not only involved in DNA repair, but is also important for maintenance of telomere, apoptosis, transcription, and recombination. These proteins are relatively abundant in the nucleus, but it can be also present in the cytoplasm (*Hu and Cucinotta, 2011*).

DNA-PKcs consists of more than 4000 amino acids. The activity of DNA-PKcs is essential for NHEJ and is thought to regulate repair pathway choice and NHEJ progression. Activation of DNA-PKcs leads to phosphorylation of many substrates (for example Ku 70/80, XRCC4, XLF, Artemis, DNA ligase IV) and itself. So far 43 phosphorylation sites of DNA-PKcs have been identified *in vitro* and *in vivo*. It has been observed that phosphorylation of DNA-PKcs pattern is different *in vitro* and *in vivo* and DNA-PKcs has two caspase cleavage sites and therefore it has been suggested that these regions are important for apoptotic processes (*Dobbs et al., 2010*). Mutations in active sites of DNA-PKcs can result in increased radiation sensitivity and increased amount of chromosomal aberrations (*Nagasawa et al., 2011*).

Artemis is a protein that can have both exonuclease and endonuclease activity. Endonuclease activity is regulated by autophosphorylated DNA-PKcs. It is known that DNA-PKcs can phosphorylate Artemis at least 11 sites. Exonuclease activity is regulated by Artemis alone. It has been shown that Artemis can process both single-stranded DNA and double-stranded DNA. If Artemis mutations cause loss of double-stranded DNA processing ability then also single-stranded DNA processing ability is lost (*Gu et al., 2010*). Artemis has been estimated to be one of the most important factors in cell cycle response to environmental stress (*Maas et al., 2010*). Other functions of Artemis include participation in apoptosis (*Britton et al., 2009*).

DNA Ligase IV consists of 911 amino acids and has a molecular weight of 96 kDa. One of the ligase IV domains binds the XRCC4 factor. Ligase IV is ATP dependent and it has been suggested that after ATP binding ligase IV changes conformation, whichis required for normal functions of protein. Mutations in the gene encoding ligase IV shows impaired DNA repair by NHEJ (*Chistiakov et al., 2009*). The function of ligase IV in NHEJ is to rejoin DNA phosphodiester backbone breaks (*Recuero-Checa et al., 2009*).

XRCC4 is a 336 amino acids long polypeptide. After purification it has been determined that most of this protein is in form of dimer with low fraction of tetramer (*Recuero-Checa et al., 2009*). DNA-PKcs phosphorylates XRCC4 mostly in two sites.

Through phosphorylation DNA-PKcs is able to regulate the ability of XRCC4 to bind DNA (*Ochi et al., 2010*). Hypersensitivity to ionizing radiation has been observed in cells that lacks XRCC4. As mentioned before XRCC4 forms complex with DNA Ligase IV and is responsible for ligation of the DSB in NHEJ pathway (*Recuero-Checa et al., 2009*).

PNK or polynucleotide kinase has molecular weight of approximately 57 kDa. This enzyme is phosphorylating the 5' end of nucleic acids and removing 3' phosphate groups (*Chappell et al., 2002*). It has been observed that decreased expression of PNK leads to cell sensitivity to ionizing radiation and extended time when H2AX is in phosphorylated form. Although PNK is required for normal functions of NHEJ it is not involved in repair process in HR or base excision repair (*Karimi-Busheri et al., 2007*). This protein is interacting directly with XRCC4 during DNA repair process (*Mahaney et al., 2009*).

The MRN complex consists of three different proteins – Rad50, Mre11, Nbs1. Mre11 relative molecular weight has been estimated to be 70-90 kDa. This protein is able to bind DNA and has endonuclease and exonuclease activity. Rad50 has relative molecular weight of about 150 kDa. It is known that Rad50 is able to bind and unwind termini of double-stranded DNA. The molecular weight of Nbs1 has been estimated to be in range from 65 to 85 kDa. Nbs1 is able to interact with repair, cell cycle checkpoint, signaling proteins and is involved in normal progress of meiosis. The interaction is mediated via phosphorylation reactions. If one of the MRN complex proteins has decreased expression then other two's expression will be also down regulated. The MRN complex takes part in DNA repair, cell cycle checkpoint activation, DNA replication, meiosis and maintenance of telomere. The actual functions of MRN complex in NHEJ are still unknown (*Lamarche et al., 2010*).

XLF is able to form homodimers and tetramers. This protein interacts with XRCC4 and affinity is estimated to be 7.8 μM. Structures of XLF homodimers are similar to XRCC4 homodimers (*Hammel et al., 2010*). Also it has been observed that purified XLF and Ku can bind each to other in presence of DNA free ends (*Yano et al., 2011*). The functions of XLF are not fully understood but it is known that XLF is involved regulation of XRCC4-DNA Ligase IV complex activity (*Malivert et al., 2010*) and

assembly of proteins for NHEJ (*Yano et al., 2011*). Mutations in XLF can cause DNA repair defects (*Malivert et al., 2010*).

DNA polymerases μ and λ are members of the X family of DNA polymerases. Polymerases are responsible for introduction of ribonucleotides and deoxynucleotides in nucleic acids. Polymerase μ is 11 times more selective for deoxynucleotides than ribonucleotides. Polymerase λ has a higher efficiency of introduction and discrimination of dNTPs than ribonucleotides (*Brown et al., 2010*). It has been suggested that there is interaction between XRCC4-Ligase IV complex and polymerase λ. Also polymerase μ is interacting directly with NHEJ components - XRCC4-Ligase IV and Ku (*Fan and Wu, 2004*). The main function of DNA polymerase is to maintain the integrity of the genome. DNA polymerases have a critical role in processes of DNA replication, DNA repair, DNA recombination and in response to DNA damage (*Ramadan et al., 2003*).

Although the sequence of protein interaction and binding during NHEJ is not fully understood several models have been suggested (also referred as alternative NHEJ). So far the best understood model states that DSB repair by NHEJ starts when Ku binds to DSBs (Figure 1 A). After binding Ku protein moves inwards - away from DNA termini making it available for interaction with other repair proteins (Figure 1 B). Then DNA-PKcs protein interacts with Ku and autoposphorylates (Figure 1 C). Some DNA-PKcs molecules interact with Artemis (Figure 1 D). It has not been established if autophosporylated DNA-PKcs dissociates from DNA termini or participates in repair complex (Figure 1 G or H). Then PNK is interacting with XRCC4-Ligase IV and this complex is recruited to DSB (Figure 1 E, F). Next step (Figure 1 G, I) involves XLF and DNA polymerases μ and λ that interacts with XRCC4-Ligase IV complex (*Mahaney et al., 2009*).

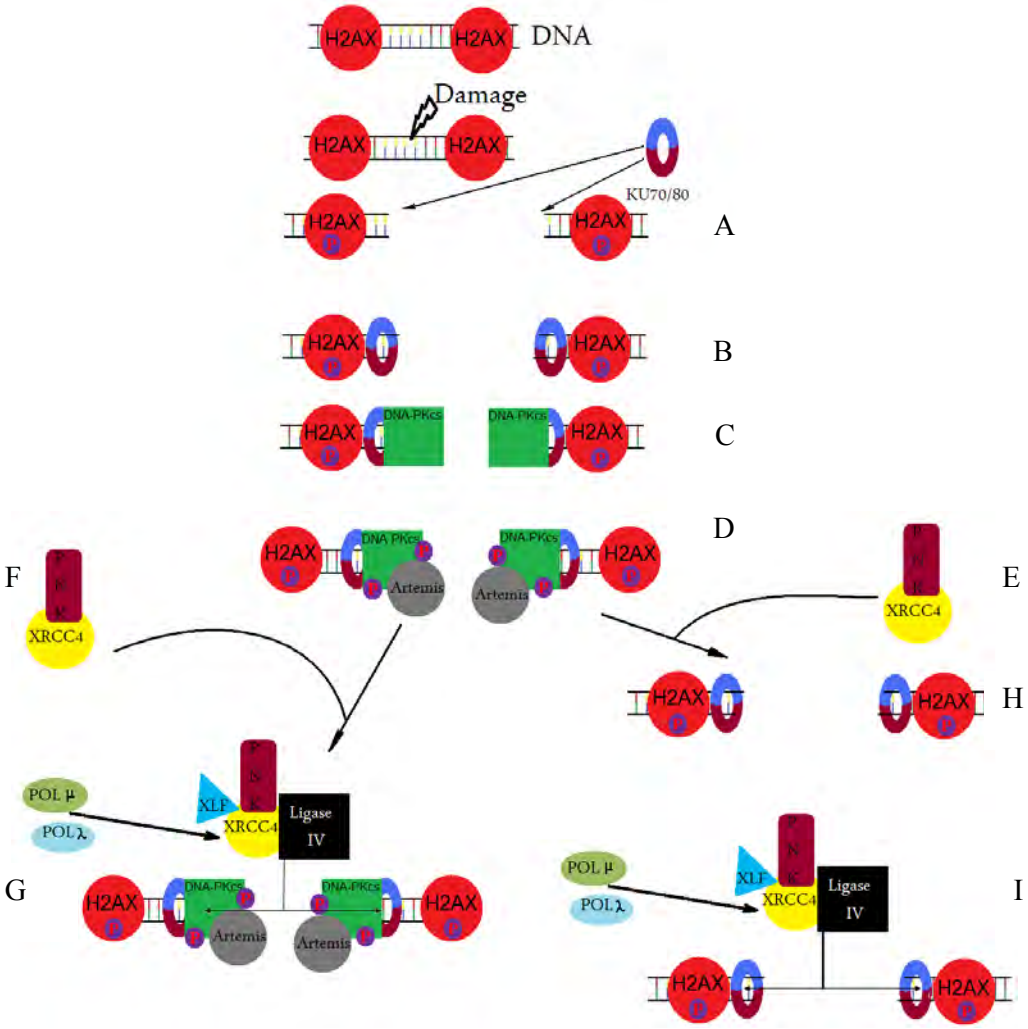

Figure 1. Schematic representation of NHEJ pathway. (A) Ku 70/80 binds to free ends of DNA. (B) Ku 70/80 moves inward. (C) DNA-PKcs interacts with Ku 70/80. (D) DNA-PKcs autophosphorylates and interacts with Artemis. (E, F) PNK binds to XRCC4. (H) DNA-PKcs dissociates form termini of DSB or (G) stays there and participates in rejoining of DSB. (I, G) XRCC4, Ligase IV, PNK and XLF complex with help from polymerases λ and μ rejoins DSB.

1.2.4. Kinetics of DSB repair

DSB repair has, at least, two phases. First estimates of DSB repair kinetics performed in CHO cells suggests that fast phase half-time is around 3.8 ± 0.9 minutes and slow phase half – time is 118 ± 30 minutes (*Dahm-Daphi and Dikomey, 1996*). It has been observed that heat-labile sites are increasing the yield of initial damage by 40% after irradiation. Therefore after exclusion of heat-labile sites half-times of fast component were reported to be 7.4 minutes and 2.5 hours for slow component (*Karlsson et al., 2008*).

1.3. Heat-labile sites

It has been suggested that heat-labile sites are damaged in the sugar backbone of DNA and requires elevated heat to transform into SSBs or DSBs. It is known that heat-labile sites can be translated into SSBs and DSBs when experiments are conducted on naked DNA. The actual mechanism for how heat-labile lesion is formed is still unknown, but it has been suggested that loss of bases combined with sugar damage make DNA molecules labile (*Rydberg, 2000*). The ability of heat-labile sites to cause DSBs in live cells is not known but it has been proposed that translation of heat-labile sites into DSB is mainly a methodological bias introduced during sample preparation for pulsed-field gel electrophoresis (PFGE) if temperature is elevated during cell lysis step (*Stenerlöw et al., 2003; Rydberg, 2000; Lundin et al., 2005*).

1.4. Methyl Methanesulfonate (MMS)

1.4.1. Mechanism of action

The DNA methylating properties of MMS has been known for decades. MMS directly interacts with adenine in positions 1, 3 and 7, guanine in positions 3, O^6 and 7, and phosphate. The methylation at position O^6 in guanine is thought to be mutagenic and referred as the general mechanism of MMS mutagenicity (*Beranek et al., 1982*). This compound has been estimated to be a relatively weak mutagen (*Glaab et al., 1999*). MMS is also regarded as S_N2-type or biomolecular nucleophilic substitution agent. S_N2 type agents have a relatively high ability to interact with nitrogen in purines and pyrimidines (*Nikolova et al., 2010*). When dsDNA (Figure 2) is exposed to MMS then 70–83% of methylations produced are 7-methylguanine, about 10% are 3-methyladenine, 2% are 7-methyladenine, 0.6% is 3-methylguanine, and 0.3% is O^6-methylguanine (*Mishina et al., 2006; Wyatt and Pittman, 2006*). Approximately 5% of methylations may occur in other position or in other base (*Wyatt and Pittman, 2006*).

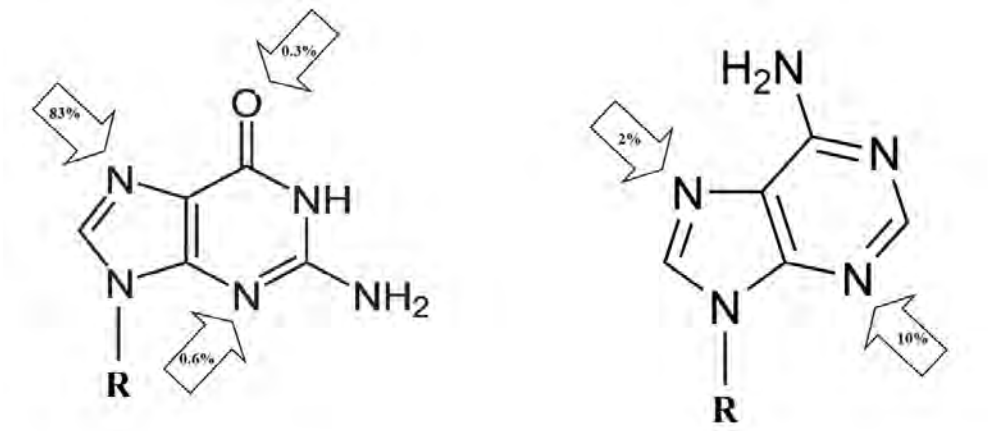

Figure 2. Methylation positions of MMS in guanine and adenine. Arrows indicate methylation positions and probability for position to be methylated.

It has been observed that MMS acts not only on nucleic acids, but also on proteins and proteins after exposure to MMS tend to acetylate. The highest amount of acetylated proteins can be observed 1 – 2 hours after treatment. Acetylation induced by MMS is reversible and reaches normal level after 12 hours after exposure. The lowest concentration reported that is able to cause protein acetylation is 50 μg/ml or 454 μM (*Lee et al., 2007*). It has been shown that MMS can induce phoshorylation of p53 and increased expression of p21 (*Jaiswal and Narayan, 2002*). Additionally MMS can also damage amino acids and tRNAs. Therefore transcriptional changes are required for recovery of damage. It has been estimated that activation of ~900 genes occurs in response of MMS damage (*Begley and Samson, 2004*). MMS is also interfering with the replication fork through blocking it (*Groth et al., 2010*). It has been observed that glutathione levels in cells have an important role in the protection mechanism against MMS-induced cell killing (*Wilhelm et al., 1997*).

1.4.2. Repair of lesions induced by MMS

Mammalian cells have different proteins that cope with damage induced by metylation – O^6 methylguanine methyltransferase (MGMT), N-methyl dioxygenases and methylpurine DNA glycosylase (*Mishina et al., 2006; Wyatt and Pittman, 2006*). MGMT is a 207 amino acids long protein and has relative molecular weight of 22

kDa. The interaction between MGMT and DNA is mediated trough the phosphate backbone of DNA. This protein is removing alkyl-adducts at O^6 position. After MGMT alkylation, it is degraded (*Mishina et al., 2006*). N-methyl dioxygenases are acting trough oxidation of the methylated cytosine at position N3 and adenine at position N1. N-methylated bases are removed by members of N-methylpurine DNA glycosylases (MPG) family. Direct removal of methylated base is conducted by BER - base excision repair. It has been shown that BER component XRCC1 (*Lundin et al., 2005*) or polymerase β deficient cell lines (*Luke et al., 2010*) are sensitive to MMS exposure. The repair of metylated phosphodiesters is still unknown. It has been estimated that these kinds of lesions are relatively harmless (*Wyatt and Pittman, 2006*).

1.4.3. Base excision repair

Different types of BER are known. Short-patch BER pathway involves removal of one damaged base while long-patch BER is processing up to 13 nucleotides (*Wilson III et al., 2010 article in press*). It has been suggested that BER modulation involves not only DNA repair proteins (*Begley and Samson, 2004*).

Short-patch BER starts when DNA glycosylase recognizes and excises a damaged base (Figure 3 A). This step leaves an abasic site. Afterwards abasic sites are processed by apurimidinic endonuclease I (APE1) or the DNA glycosylase (Figure 3 B). Then DNA ends are modified and DNA ends with 3'OH and 5'P are created. The next step involves nucleotide insertion by DNA polymerase β (Figure 3 C). Mutations can be induced during this process if ligation happens before nucleotide insertion. Ligation of DNA ends (Figure 3 D) in short-patch BER is processed by DNA ligase IIIα (*Nemec et al., 2010; Wilson III et al., 2010 article in press*). XRCC1 is a prominent protein for short-patch BER. Interaction between XRCC1 and polymerase β and Ligase III has been observed. It is thought that XRCC1 is acting as scaffold protein (*Robertson et al., 2009*).

Long-patch BER and short-patch BER has the same first two steps (Figure 3 A and B). Then polymerase β or polymerase Δ displaces more than one nucleotide (Figure 3 E). Afterwards flap specific-endonuclease 1 (FEN1) removes the flap generated by

the polymerases (Figure 3 F). FEN1 is important for normal functions of long-patch BER and without FEN1 the long-patch BER is not functional. Then ligation is carried out by the DNA ligase I (Figure 3 G). Also long-patch BER requires protein – PCNA. PCNA is necessary for FEN1 and polymerase Δ functions in long-patch BER (*Robertson et al., 2009*).

Although the choice of selection between long-patch and short-patch BER pathways are not known several hypothesis have been suggested. One of these theories implies that selection of long-patch or short-patch BER is the result of relative ATP concentration around the abasic site. In low ATP regions long-patch BER is favored. The second theory suggests that successful removal of 5'dRP by polymerase β leads to short-patch BER (*Robertson et al., 2009*).

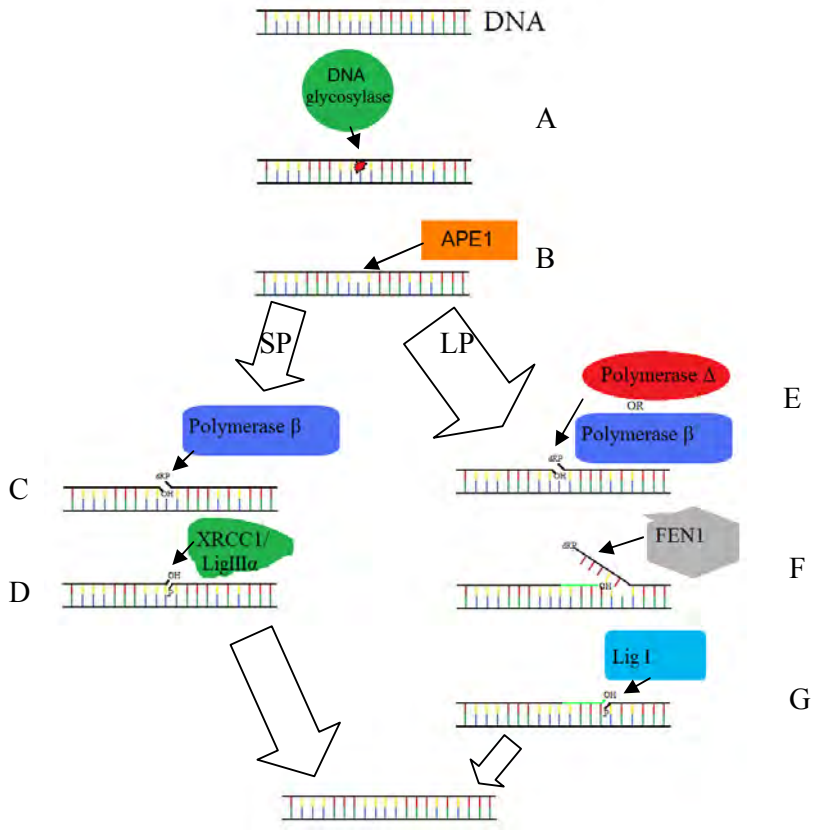

Figure 3. Base excision repair starts when DNA glycosylase detects damaged base and excise it (A). Then APE1 modifies DNA ends creating 3'OH and 5'P (B). Afterwards the choice between short-patch (SP) and long-patch (LP) BER is made. In short-patch BER dR is removed and a nucleotide is inserted by polymerase β (C). Ligation of DNA ends is processed by XRCC1 and Ligase IIIα (D). In long-patch BER polymerase β or polymerase Δ inserts more nucleotides (E), therefore creating a flapped structure. The flap is then removed by FEN1 (F) and the ligation processed by Ligase I (G).

Efficiency of BER is determined by position where damage is induced. There are at least 11 different DNA glycosylases that are showing substrate specificity (*Robertson et al., 2009*). Therefore the ability of DNA glycosylase to recognize damaged base and excise it is limiting the speed of BER. This statement is also supported by the fact that AP site repair occurs faster than the formation of an AP site. Another factor that influences repair speed of BER is poly(ADP-ribose) polymerase 1 (PARP1). Although it is not directly participating in BER it can directly interact with BER proteins and regulate their functions (*Allinson et al., 2004*).

1.4.4. MMS induced DSBs

It has been thought that MMS induces DSBs in an indirect way. The experiments with S-phase cells have shown that increase of γH2AX foci can be observed after exposure to MMS. No increase of γH2AX foci could be observed in G0 and G2 cells. As an explanation of these data it has been suggested that DSBs induced by MMS are result of a collapsed replication fork (*Nikolova et al., 2010; Groth et al., 2010*), although it is not ruled out that MMS cannot induce DSBs in G0 or G2 phase cells, relatively high alkylation levels would then be required. As a result, a high amount of SSBs are created by BER that could be converted into DSBs if it occurs closely on opposite sides of DNA (*Nikolova et al., 2010*).

It has been estimated that DSBs induced by MMS in S-phase are repaired by HR and not by NHEJ. The data from colonogenic survival assays shows that cells that have compromised NHEJ are relatively resistant to MMS. But cells with impaired BER or HR are more sensitive to MMS treatment (*Nikolova et al., 2010*).

2. MATERIALS AND METHODS

2.1. Cell cultivation and lines

Wild-type DNA-PKcs glioma-derived cell line - M059K and glioma-derived cell line deficient in DNA-PKcs - M059J (*ATCC, Manassas, VA, USA*) monolayer were grown in DMEM (Dulbecco's Modified Eagle's media) / F-12 (Ham's F-12 nutrient mixture) in ratio 1:1 media (*Biochrom KG, Germany*) that was supplemented with 10% fetal bovine serum (*Sigma, Germany*), 1x non essential amino acids (*Biochrom KG, Germany*), 1% penicillin/streptomycin (*GIBCO*) and 2 mM L-glutamine (*Biochrom KG, Germany*). Normal human skin-derived fibroblast cells GM5758 (*Human Genetic Mutant Cell Repository, Camden, USA*) monolayers were grown in EMEM (Eagle's minimum essentials medium, *Biochrom KG, Germany*). Human colon cancer deficient in Mre11 - HCT116 (*ATCC, Manassas, VA, USA*) and Chinese hamster ovary cells, deficient in XRCC1 – EM9 (*provided by Thomas Helledey*) monolayers were grown in DMEM/F-12 media.Media for EM9, HCT116 and GM5758 were supplemented with 2 mM L-glutamine, 1% penicillin/streptomycin and 10% fetal bovine serum. Cells were incubated in 5% CO_2 and 95% air environment at 37^{o}C.

2.2. Chemicals and treatment

A 7 mM stock of the DNA-PKcs inhibitor NU7026 (*Calbiochem, USA*) was prepared in DMSO (*Merck, Germany*) and stored at - 20°C. In PFGE experiments when DNA-PKcs inhibitor was used cells were pre-treated for 1 hour with 50 μM NU7026 in complete media at 37°C. Controls, when NU7026 was used, were also treated with inhibitor. During irradiation or MMS treatment NU7026 was present in media.

The methylating agent methylmethane sulfonate (MMS) was prepared as 11.8 M stock solution in deionized water (kindly provided by Thomas Helleday). The stock was stored at 4°C. Before every treatment fresh 0.1 M MMS solution was prepared in 1X PBS that was diluted in complete media to final concentration of 1, 2, 3, 4, 5 and 10 mM for PFGE or 1 mM for immunocytochemistry. For all experiments 1h incubation at 37°C of appropriated dose of MMS was used. After treatment media

containing MMS was removed and cells were washed once with 1X PBS. Then new preheated complete media was added.

2.3. Irradiation

Cell irradiation was used for PFGE assay and immunocytochemistry as a positive control. For PFGE, cells were put on ice for at least 25 minutesbefore irradiation. For repair time 0 minutes and controls cells were embedded in low gelling point InCert (*BMA, USA*) 0.6% agarose plugs prior irradiation. Cells were irradiated with ^{137}Cs γ-ray photons (Gammacell 40 Exactor, *MDS Nordion, Canada*) at a dose rate 1.04 Gy/min. Cells for PFGE were irradiated on ice with 40 Gy and for immunocytochemistry at room temperature with 2 Gy.

2.4. Pulsed field gel electrophoresis (PFGE)

For pulsed field gel electrophoresis 40 000 of HCT116, 20 000 or 30 000 (for confluent dish) of M059J and 20 000 of M059K cells were seeded in 35 mm petri dishes. Complete media with 2 kBq of [14C]thymidine (*PerkinElmer, USA*)was added for at least two cell doubling times.

After irradiation the cold medium was replaced with 37^{o}C media containing the same amount of NU7026. Cells treated with 3 mM MMS for 1 hour were washed once with PBS and warm complete media or complete media containing the same amount NU7026 was added. Then cells were trypsinised in 150 µl for 5 – 7 minutes. Then 150 µl of low-gelling-point InCert agarose was added. Two plugs were prepared from each dish representing cold and warm lysis protocols. Volume of each plug was 100 µl. After preparation each plug was placed on ice for 20 – 30 minutes. The time when plugs were placed on ice was assumed as end of repair. After gelling of agarose all plugs were transferred into lysis buffer.

Two different lysis temperatures were used – 50^{o}C (warm lysis) and 4^{o}C (cold lysis) as described earlier [14]. For warm and cold lysis ESP-buffer was used. It contained 0.5 M EDTA pH 8 (*Aldrich, USA*), 2% N-lauroylsarcosine (*Sigma-Aldrich, UK*), approximately 1 mg/ml proteinase K (*Roche Diagnostics GmbH, Germany*). Then plugs for warm lysis were placed in 50^{o}C for 18 hours while plugs for cold lysis were

left in 4°C. All samples were lysed at least 24h in ESP-buffer. After this step warm and cold lysis plugs were treated in the same manner. All plugs were put in HS-buffer that contained 1.85 M NaCl, 0.15 M KCl, 5 mM $MgCl_2$, 2 mM EDTA, 4 mM Tris, 0.5% Triton X–100, pH 7.5. Then samples were incubated for 20 hours in 4°C. Afterwards plugs were washed twice in 0.1 M EDTA for 1 hour each time and once for one hour in 0.5X TBE (44.5 mM Tris (*Sigma-Aldrich, China*), 44.5 mM boric acid (*Merck, Germany*) and 1 mM EDTA).

Agarose plugs prepared for time dependence of conversation of heat-labile sites to DSBs were first lysed at least for 24 hours in ESP buffer and then followed 20 hours incubation in HS buffer. Afterwards plugs were washed 3 times with 0.5 M EDTA. Then tubes were transferred in heating block (*Hybridisation oven, Amersham, UK*) and incubated at 50°C for 1, 2, 4, 18 and 24 hours. After incubation plugs were washed twice with 0.1 M EDTA for 1 hour each time followed by final wash in 0.5X TBE for 1 hour.

The plugs were loaded in pre cooled 4°C, agarose gel (*0.8%*, *SeaKem Gold*, *BMA*, *USA*). Afterwards all wells were sealed with 0.8% agarose gel and placed for 1 hour in PFGE unit (*Pharmacia Biotech*, *Sweden*) that was filled with 0.5X TBE. DNA was separated using 56 volts and five pulses – 3 hours with 10 minutes pulses, 5:20 hours with 20 minutes pulses, 8 hours with 30 minutes pulses, 9:20 hours with 40 minutes pulses and 20 hours with 60 minutes pulses. The temperature during electrophoresis was 10°C. Then gel was removed from PFGE unit and placed in ethidium bromide 1 mg/l at least for two hours. Afterwards the gel was destained in water for 2 hours. As DNA ladder *S. pombe* (*BMA, USA*) chromosomes were used. Afterwards the gel was sliced in two pieces – fragments > 5.7 Mbp and fragments < 5.7 Mbp. Slices then were put in scintillation vials. Two ml of deionized water were added to gel slices containing fragments <5.7 Mbp. Then in all vials 1 ml of 0.2 M HCl (*Merck, Germany*) was added. Afterwards all samples were put in heater (*Ehret, Germany*) in 95°C for 1-1.5 hours. When samples were cooled down to room temperature 5 ml of scintillation liquid (*Quicksafe A, Zinsser Analytic, UK*) was added. At least 12 hours after addition of scintillation liquid the ^{14}C amount was measured with a liquid scintillation counter (*Wallac Betarack*, *Finland*). Count time for each sample was 600 seconds. Obtained counts were then processed with Microsoft Excel and

GraphPadPrism 5.0. Before plotting, data were normalized to level of first time point. Exponential curves and sigmoidal dose-response curves (built in functions in GrapPadPrism) were fitted to data points.

For separation of smaller DNA fragments pre-cooled gel of 1% agarose dissolved in 0.5X TBEwas used. Then plugs were loaded in wells and they were sealed using the same concentration of agarose. Before starting separation gel was left in the electrophoresis box for 1 hour. The procedure for PFGE separation involved three different pulse lengths – 10 seconds for 7 hours, 40 seconds for 5 hours and 70 seconds for 5 hours. Then staining with ethidium bromide and destaining was performed as described before. Afterwards gel was sliced in nine different pieces. Fragments included DNA sizes from 0–48.5, 48.5–97, 97-145.5, 145.5–225, 225–375, 375–680, 680–930, 930–1110 and >1110 kbp. Fragment sizes were determined using *S. cerevisiae* (*Cambrex, USA*) and *Lambda* DNA-PFGE (*Lonza, USA*) markers. Then all gel slices were relocated to scintillation vials and volume were equalised using deionised water. Afterwards 0.2 M HCl was added to all samples that were treated and analyzed as described before.

2.5. Immunocytochemistry

For immunocytochemistry a drop containing cells were put on glass slides. When cells were attached to the surface (after approximately 2 hours), appropriate media were added. After reach of repair time, the glass slides were washed in PBS and fixed in 99% ice cold methanol (*Merck, Germany*) for 20 minutes. Then the glass slides were dipped in 4°C cold acetone (*Solveco, Sweden*) for 15 seconds. After three times wash in 1XPBS for 5 minutes each time, cells were blocked in 10% FBS in room temperature for 1 hour. Primary mouse antibodies against phosphorylated DNA-PKcs (*Abcam, United Kingdom*) and rabbit against 53BP1 (*Bethyl Laboratories, USA*) was diluted in ratio 1:100 in 1% FBS and incubated at 4^{o}C overnight. Then glass slides were washed three times for 5 minutes each wash in PBS. Secondary antibodies Alexa Fluor anti-rabbit donkey (*Invitrogen, USA*) and anti-mouse goat (*Invitrogen, USA*) antibodies in ratio 1:400 were diluted in 1% FBS. Glass slides were covered with secondary antibody solution and incubated at room temperature for one hour. Afterwards all samples were washed three times for 5 minutes each time with PBS.

Then slide were stained with 0.1 μg/ml DAPI (*Sigma*) for 2 minutes. Unbound DAPI stain was removed by once washing slide in PBS for 10 minutes and then rinsed with water. Then slide were covered with mounting media (*Vectashield, Vector Laboratories Inc, USA*) and cover-slips. Pictures were captured using Zeiss LSM 510 Meta (*Carl Zeiss, Germany*) 63x or 40x magnification oil immersion objective. Images were captured as stacks and afterwards merged. Then pictures were processed by ImageJ.

3. RESULTS

3.1. Optimization of heat-labile site induction conditions and damage pattern

To determine optimal MMS exposure dose for PFGE experiments, M059J cells were used. From these data (Figure 4) it is possible to observe that MMS in concentrations 1 – 5 mM, DNA is intact when cells were lysed at 4°C. On contrary, when samples were lysed at 50°C, the number of detected DSBs increased with increasing MMS concentration. For data points presenting lysis protocol at 50°C sigmoidal dose-response curve was fitted (R^2 = 0.9968). At the high concentration (10 mM),a small amount of DSBs were also detected after cold lysis.

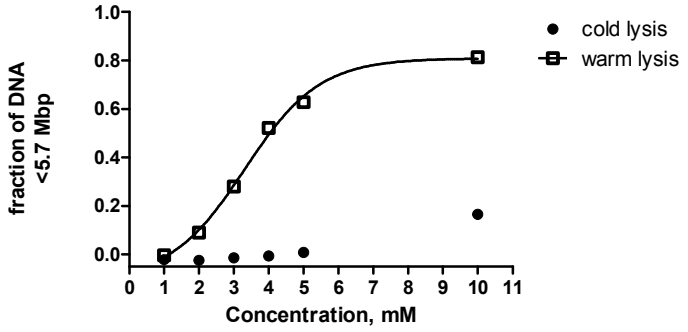

Figure 4.Induction of DSBs in M059J cells after exposure to increasing concentration of MMS. Cells were treated with MMS for 1h at 37°C and then agarose plugs were prepared. Samples were then treated with cold lysis or warm lysis before separation with PFGE. Sigmoidal dose-response curve were fitted to warm lysis data points. Data from one experiment is shown.

Next experiment was conducted to understand the impact of cell density on repair process of lesions induced by MMS (Figure 5). It was observed that there is no difference of heat-labile sites in the range of 1 hour after treatment. A clear difference was observed after 4 hours where cells form confluent dishes showed continuous decrease of heat-released DSB (warm lysis) and small increase of DSBs (cold lysis). But cells from non-confluent exhibited approximately 10 fold increase of DSBs and followed increase also in heat treated sample.

Small fragment analysis with PFGE (Figure 6 A) shows that warm lysis treated sample with 3 mM MMS for 1 hour has elevated amount of DNA fragments in region in between 1100 kbp and 375 kbp compared to control. After 375 kbp border lower

levels of DNA can be detected. In contrast cold lysis treated cells for the same time point shows increased amount of DNA less than145.5 kbp in size(Figure 6 B).

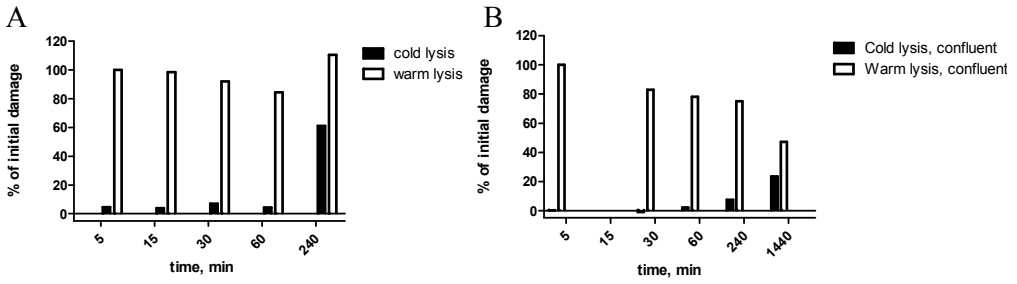

Figure 5. M059J cells were treated with 3 mM MMS for 1 hour. After washing, the cells were incubated in fresh medium without MMS for the stated times and then prepared for PFGE analysis using cold and warm lysis.Results of confluent dish and (B) non-confluent dish are presented. Data normalized to 5 minutes repair time and data represents one experiment.

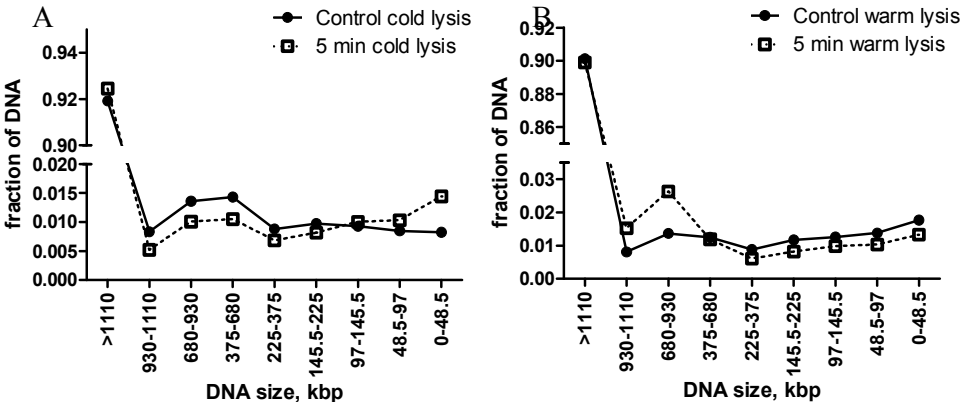

Figure 6.Small DNA fragment analysis with PFGE of 3 mM/h treated M059J cells using (A) cold lysis and (B) warm lysis. Repair time 5 minutes after change of medium is presented in comparison with controls. Data from one experiment is shown and line joining data points are fitted with eye.

3.2. Repair of heat-labile sites induced by MMS and IR

To further reveal how heat-labile sites are repaired, HCT116 cells with wild-type NHEJ were used. Data obtained from PFGE assay shows that repair of MMS induced heat-labile sites in HCT116 is relatively slow process (Figure 4).In first 30 minutes almost no repair can be observed. After 1, 4 and 24 hour of repair approximately 82%, 72% and 20% of the initial damage was detected. Removal of ionizing radiation (IR) induced heat-labile sites in M059K (Figure 5) in comparison is a relatively fast process. After 15 minutes of repair more than 50% of induced heat-labile sites are

repaired. One hour after irradiation there are no unrepaired heat-labile sites left (Fiugre 7 and 8).

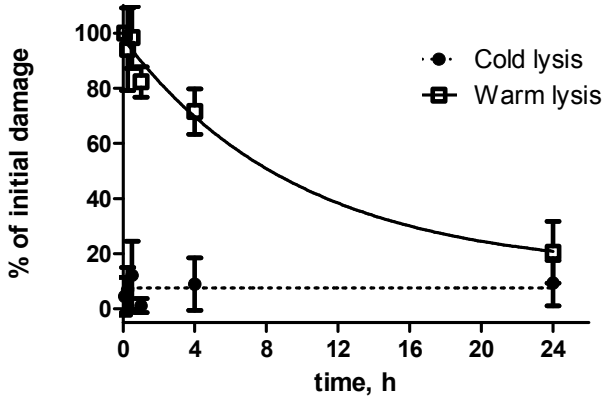

Figure 7. Repair of heat-labile sites induced by 3 mM MMS treatment for 1 hour in HCT116 cells. All datapoints are normalised to first point (5 minutes). Amount of unrepaired heat-labile sites were detected at 15, 30, 60, 240 and 1440 minutes after removal of media containing MMS. Data from two to three independent experiments are shown. Exponential function is fitted for datapoints. Error bars represent standart deviation.

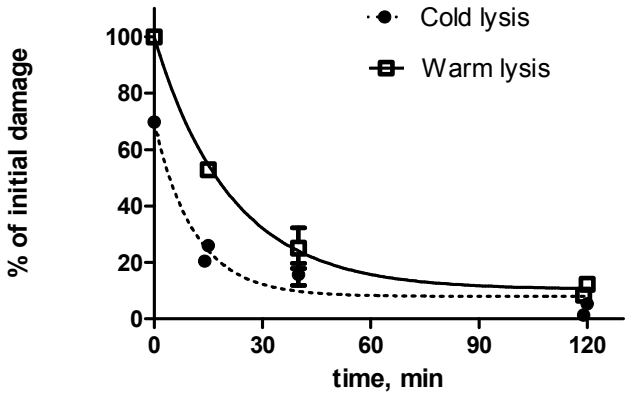

Figure 8. Rejoining of DSBs and repair of heat-labile sites in M059K cells after irradiation with 40Gy of photons. Repair at 15, 40 and 120 minutes are presented. Data from two independent experiments are shown. Exponential functions are fitted to data points. Data normalised to levels of heat-labile damage at repair time 0.

Inhibition of DNA-PKcs by NU7026 did not show any effect on repair capacity of heat-labile sites induced by MMS (Figure 9). Repair of 21% and 32% was observed at 1 hour and 4 hour repair time points which was smaller to cells without NU7026 (that is 3 and 4% more damage removed at the same time points).

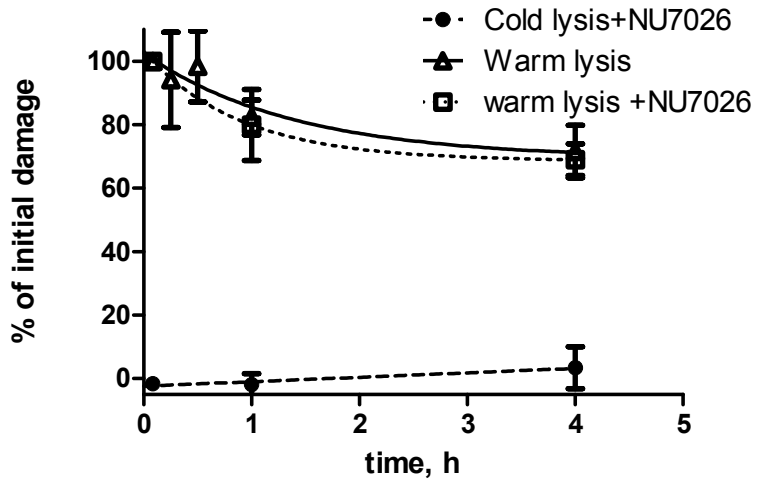

Figure 9. Repair of heat-labile sites introduced by 3 mM/h MMS after inhibition of NU7026 in HCT116 cells. Amount of unrepaired heat-labile sites were detected at 15, 30, 60, 240 and 1440 minutes after removal of media containing MMS.Datapoints are normalised to first point (5 minutes). Data represented by empty triangeles are taken form Figure 7. Data from 3 independent experiments are shown and exponential function is fitted to the data points.

The efficiency of NU7026 inhibit rejoining of DSBs induced by IR was determined at 4 hours and 24 hours (Figure 10).From obtained data it is possible to observe that approximately 65% of DSBs are unrepaired at 4 hours and is around 78% at 24 hours. Also after 4 hours no difference between cold and warm lysed sample can be detected.

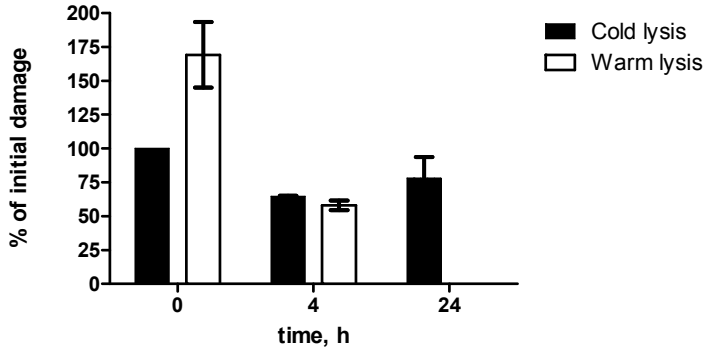

Figure 10. Efficiency of NU7026 to inhibit rejoining of DSBs caused by 40 Gy IR in HCT116. Data normalised to the levels of cold lysis treated sample at repair time point 0. Two to four independent experiments were conducted. Error bars represent SD.

3.3. Transformation of heat-labile site into DSB

Transformation of heat-labile sites into DSBs is strongly dependent on time and temperature. To analyze if the kinetics of this transformation is different depending on the heat-labile site inducing agent, the conversation of heat-labile sites into DSBs at 50°C was studied after IR and MMS treatment (Figure 11). Transformation of heat-labile sites into DSBs was much faster in the first 4 hours in cells treated with IR, compared to those treated with MMS. Heat-labile sites induced by MMS were following quadratic equation with heat-labile sites introduced by IR could be characterized by logarithmic equation. Approximately 4 hours was required for 50% IR induced heat-labile sites to transform into DSBs compared to the amount of DSBs observed after 18 hour incubation. On contrary, in the first 4 hours only 8% of heat-labile sites induced by MMS are modified.

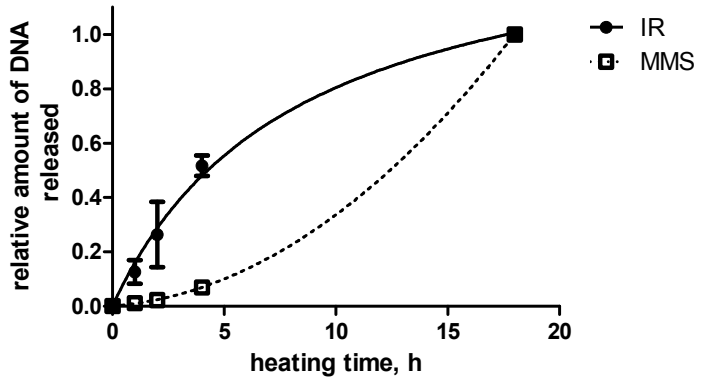

Figure 11. Ionizing radiation and MMS induced heat-labile site transformation into DSBs after incubation at various times in 50°C. Cells were treated with 40 Gy (gamma radiation) or 5 mM MMS for 1 hour. Plugs were lysed in ESP buffer for at least 24 hours at 4°C and then transferred into HS buffer for 18 hours. Then all plugs were washed trice with 0.5 M EDTA. Samples were heated for 0, 1, 2, 4 and 18 hours in 0.5 M EDTA. Afterwards cells were washed with 0.5X TBE and PFGE was performed as described before. HCT116 cells were used in experiment and data from two independent experiments are shown. Quadratic curve is fitted to MMS data points and logarithmic to IR data points. Error bars represent SD.

3.4. Immunocytochemistry

To further reveal if heat-labile sites result in DSB-response activation, cells were stained with DSB – markers using immunocytochemistry. Positive control of HCT116 cells irradiated with 2 Gy and 1 hour repair time showed clearly distinguishable

53BP1 foci that colocalised with phosphorylated DNA-PKcs (Figure 12 A). Several relatively large foci could be observed also in non-treated cells (Figure 12 B). After exposure to 1 mM MMS for 1 hour, foci count increase but there were still some cells with no foci (Figure 12 C). After 1 and 4 hours of repair most of the cells still had foci (Figure 12 D and E).

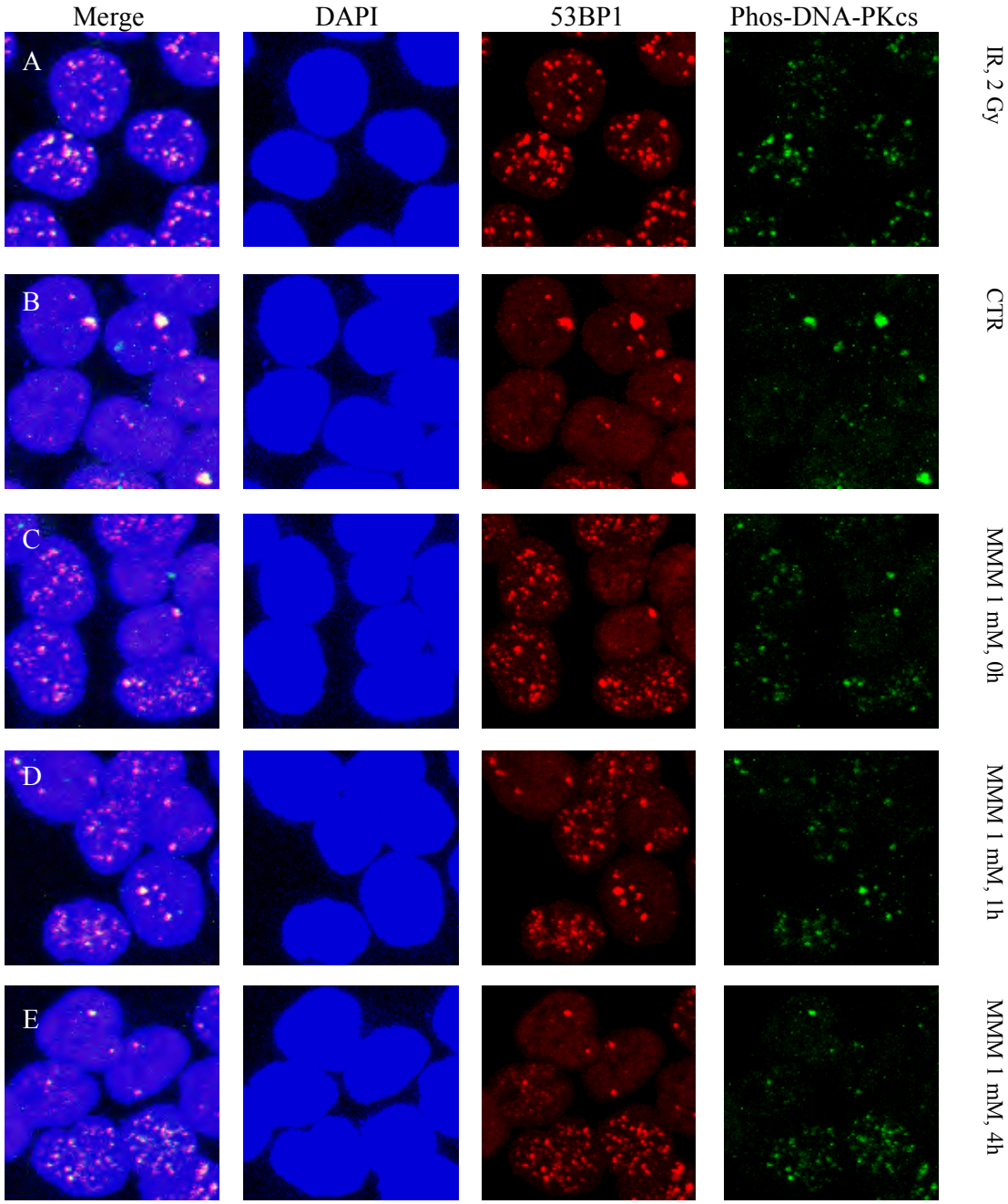

Figure 12. Foci formation in HCT116 cells after exposure to 2 Gy of IR and 1 hour repair(A), controls (B) or 1 mM MMS exposure and repair 0 (C), 1 (D) and 4 hours (E). Red channel represents 53BP1, green – phos DNA-PKcs, blue – DAPI.

In contrast to HCT116 cells normal human fibroblasts GM 5758 showed no foci formation in controls (Figure 13 B). In fibroblastsfewer cells contained nuclei contained fewer cells with 53BP1 and phosphorylated DNA-PKcs foci at any time point (Figure 13 C - E). In fibroblast positive control (2 Gy IR and 1 hour repair) approximately the same amount of foci were formed as in HCT116 cell positive control (Figure 13 A).

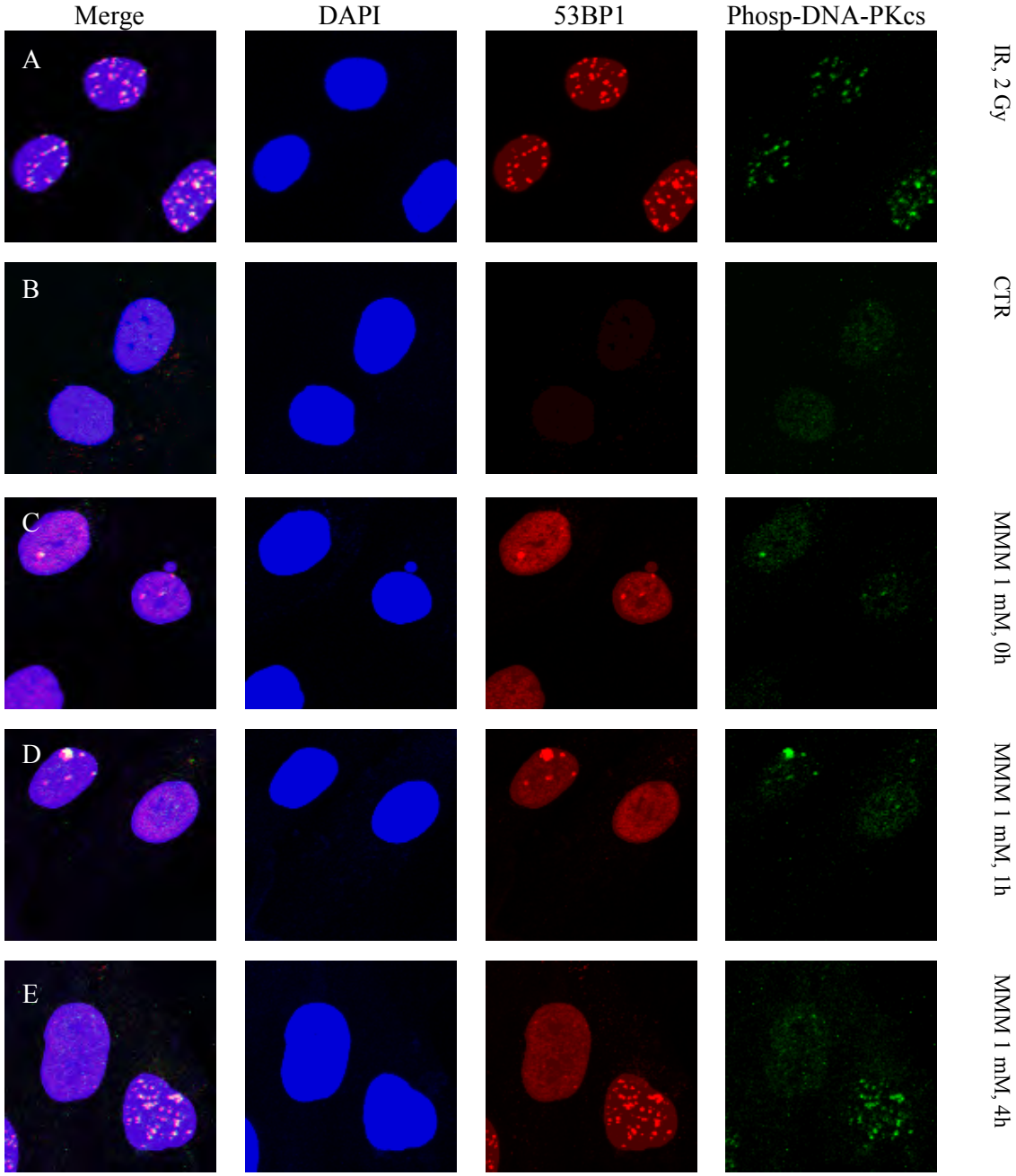

Figure 13. Foci formation in GM5758 cells after exposure to 2 Gy of IR and 1 hour repair(A), controls (B) or 1 mM MMS exposure and repair 0 (C), 1 (D) and 4 hours (E). Red channel represents 53BP1, green – phos DNA-PKcs, blue – DAPI.

The XRCC1 deficient hamster cell line EM9 showed activation of DNA-PKcs and formation of foci that less colocalized with 53BP1 foci (Figure 14 C, D) in comparison with human cell lines (Figure 12 - 13). Although positive control showed the same colocalisation pattern (Figure 14 A) that is observed in human cell lines after 2 Gy irradiation and 1 hour repair. Also no colocalised formation of foci could be observed in control sample (Figure 14 B).

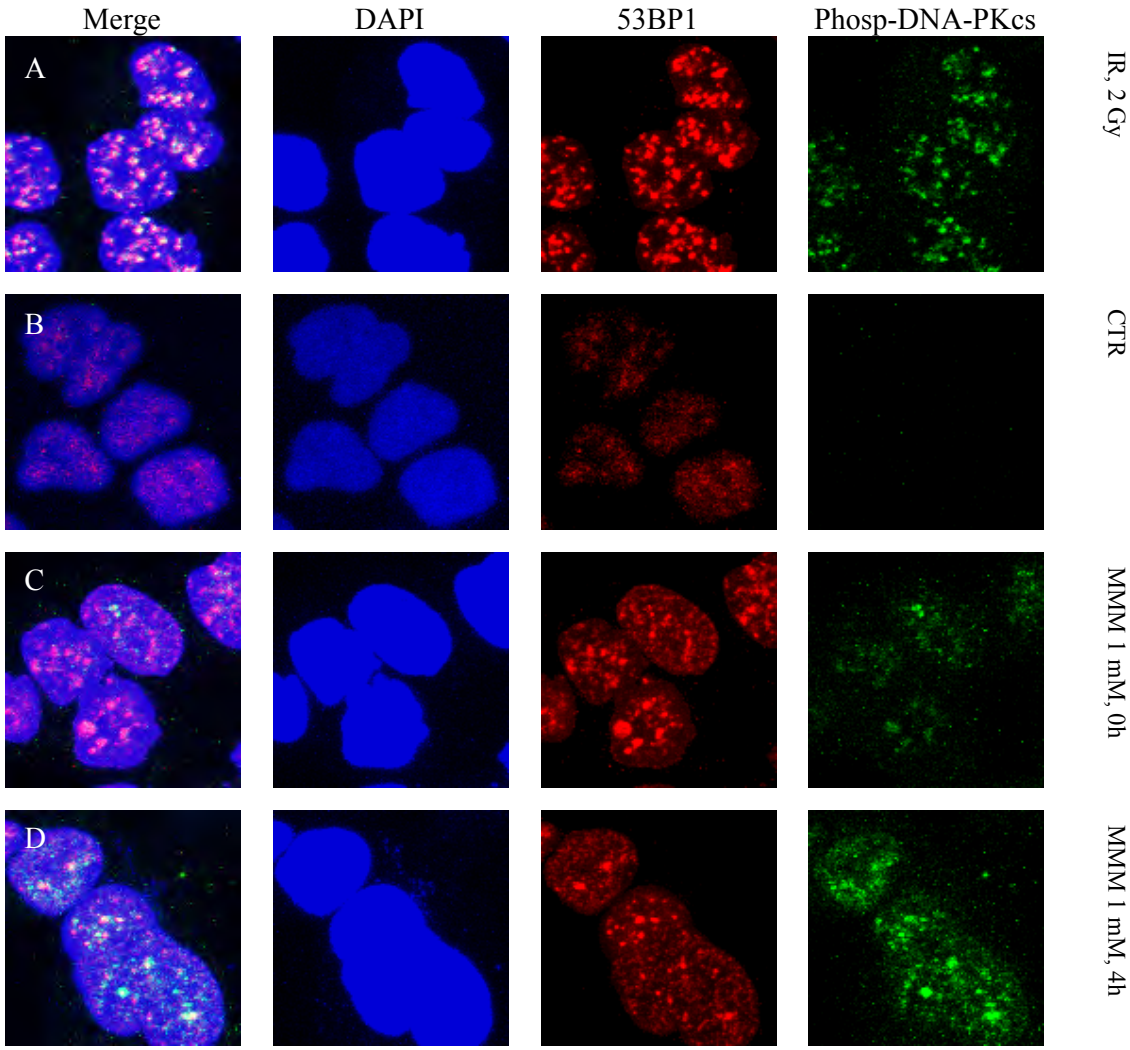

Figure 14. Foci formation in EM9 cells after exposure to 2 Gy of IR and 1 hour repair(A), controls (B) or 1 mM MMS exposure and repair 0 (C) and 4 hours (D). Red channel represents 53BP1, green – phos DNA-PKcs, blue – DAPI.

4. DISCUSSION

4.1. Optimization and experimental settings

Although experiment for optimization of drug exposure concentration was performed only once, the obtained results showed good correlation between data points. Afterwards 3 mM exposure for 1 hour was chosen to be used in following experiments for PFGE. Additional test for the ability of 3 mM/h MMS exposure to induce damaged DNA was performed and transformation of small DNA fragmentswas analyzed by the PFGE assay. Data from this experiment showed only small increase of fragments between 0 - 48.5 kbp in cold lysis treated samples at early time points. Therefore no considerable toxic effects can be expected at early time points. Incubation time (18 hours) for transformation of heat-labile sites into DSBs was used because it was reported that there is no increase of IR induced heat-labile site modifications to DSBs after 15 hours (*Stenerlöw et al., 2003*). In another report 48 h incubation at 50°C was used for conversation of heat-labile sites to DSBs after exposure to MMS (*Lundin et al., 2005*). Even if all heat-labile sites were not converted into DSBs it did not affect the results because all samples were treated in the same manner and data were afterwards normalized to the levels of the first data point.

The confluence of cells during MMS exposure had a great importance for late effects that were not observed one hour after exposure. Therefore data suggests that cycling cells are more affected than non-cycling cells. This statement is in agreement with previous studies with hamster cells (*Nikolova et al., 2010; Groth et al., 2010*).

4.2. Involvement of NHEJ in MMS induced heat-labile site repair and heat-labile site repair kinetics

Data for PFGE experiments reported slow removal of heat-labile sites induced by MMS and fast removal of heat-labile sites induced by IR. Similar removal rate of MMS induced lesions was reported by using comet assay in human colon cancer cells RKO(*Jung et al., 2009*). Repair kinetics of heat-labile sites induced by IR and MMS suggest that these lesions are different in nature.

Inhibition of DNA-PKcs did not have an effect of heat-labile sites induced by IR and MMS. If DNA-PKcs was important for the repair of heat-labile site, the kinetics should change. However, there was no difference in heat-labile site removal between non-treated cells andtreated cells with DNA-PKcs inhibitor. The inhibition efficiency increase determined at the 24 hour time point might be a result of the start of apoptotic processes as DNA-PKcs deficient cell line in the first 4 hours shows the same repair capacity as DNA-PKcs proficient. The difference of damage amount observed at 24 hours between HCT116 and M059J can be explained by the fact that lack of DNA-PKcs facilitates apoptosis in response to DNA damage (*Gurley et al., 2009*). It is possible to speculate that slow removal of methylated bases involving BER is a cell defense mechanism against two opposite sided SSBs formation in proximity therefore causing DSB.

Immunocytochemistry showed activation of DNA-PKcs by autophosphorylation at position 2609. As phosphorylated DNA-PKcs foci colocalized with the DSBs marker 53BP1 it is possible to suggest that direct involvement of NHEJ is required to repair lesions induced in DNA by MMS. But on the other hand it is known that DNA-PKcs is able to phosphorylate histone H2AX (*Park et al., 2003*). Therefore access of repair proteins to damaged site is facilitated. The fact that the XRCC1 deficient cell line EM9 exhibited lower amount of DNA-PKcs activation and lesser phosphorylated DNA-PKcs colocalization with 53BP1 could be explained by differences in repair processes between human and hamster cells. It has been shown that DNA-PKcs deficient hamster cells are able to rejoin DSBs while human cells deficient in DNA-PKcs cannot (*Karlsson and Stenerlöw, 2007*). The data acquired in this study is in conflict with conclusions done by Nikolova et al. (*2010*) and showed that activation of prominent protein involved in NHEJ happens after exposure to MMS in human and hamster cells.

4.3. Kinetics of heat-labile site transformation into DSBs

Experiment revealing kinetics of heat-labile site transformation into DSBs showed that IR and MMS induced heat-labile sites are modified at different speeds. As repair and modification of heat-labile sites are different between IR and MMS treated samples then data suggests that there are more than one type of heat-labile sites and

IR and MMS induced heat-labile sites are not related. Generally high temperatures and long time of heating is required for heat-labile sites to become modified. Therefore the probability of heat-labile sites transform directly in DSBs *in vivo* can be estimated as very low. Unless it happens in replicating cell or high amount of heat-labile sites are introduced or by chance if closely spaced modification of base on opposite strands of DNA is repaired simultaneously.

5. CONCLUSIONS

1. Chemically induced heat-labile sites are different form ionizing radiation induced ones.

2. In response to MMS treatment DNA-PKcs autophosphorylation can happen.

3. Involvement of NHEJ in heat-labile site repair induced by chemical agent is still unclear.

6. ACKNOWLEDGEMENTS

The study was performed at Department of Biomedical Radiation Sciences, Uppsala University. Many employees at BMS have directly or indirectly helped to complete this study. I would like to express special gratitude to my supervisor Prof. Bo Stenerlöw for accepting me in his research team, for advice and his devoted time in discussions. Many thanks also for PhD student Ann-Sofie Gustafsson for help to capture pictures.

REFERENCES

Allinson SL, Sleeth KM, Matthewman GE, Dianov GL. 2004. Orchestration of base excision repair by controlling the rates of enzymatic activities. *DNA repair 3*, 23 – 31.

Begely TJ and Samson LD. 2004. Network responses to DNA damaging agents. *DNA repair 3*, 1123 – 1132.

Beranek DT, Heflich RH, Kodell RL, Morris SM, Casciano DA. 1982. Correlation between specific DNA-methylation products and mutation induction at the HGPRT locus in Chinese hamster ovary cells. *Mutation Research 110*, 171 – 180.

Bohgaki T, Bohgaki M, Hakem R. 2010. DNA double-strand break signaling and human disorders. *Genome Integrity 1:15*.

Britton S, Frit P, Biard D, Salles B, Calsou P. 2009. Artemis Nuclease Facilitates Apoptotic Chromatin Cleavage. *Cancer Research 69,* 8120 – 8126.

Brown JA, Fiala KA, Fowler JD, Sherrer MS, Newmister SA, Duym WW, Suo Z. 2010. A Novel Mechanism of Sugar Selection Utilized by a Human X-Family DNA Polymerase. *Journal of Molecular Biology 395,* 282 – 290.

Chappell C, Hanakahi LA, Karimi-Busheri F, Weinfeld M, West SC. 2002. Involvement of human polynucleotide kinase in double-strand break repair by non-homologous end joining. *The EMBO Journal 21*, 2827 – 2832.

Chistiakov DA, Voronova NV, Chistiakov AP. 2009. Ligase IV syndrome. *European Journal of Medical Genetics 52,* 373 – 378.

Dahm-Daphi J and Dikomey E. 1996. Rejoining of DNA double-strand breaks in X-irradiated CHO cells studied by constant-and graded-field gel electrophoresis. *International Journal of Radiation Biology 69*, 615 – 621.

Dobbs TA, Tainer JA, Lees – Miller SP. 2010. A structural model for regulation of NHEJ by DNA-PKcs autophosphorylation. *DNA repair 9*, 1307 – 1314.

Falk M, Lukasova E, Kozubek S. 2010. Higher-order chromatin structure in DSB induction, repair and misrepair. *Mutation Research 704,* 88 – 100.

Fan W and Wu X. 2004. DNA polymerase λ can elongate on DNA substrates mimicking non-homologous end joining and interact with XRCC4-ligase IV complex. *Biochemical and Biophysical Research Communications 323*, 1328 – 1333.

Frankenberg-Schwager M, Gebauer A, Koppe C, Wolf H, Pralle E, Frankenberg D. 2009. Single-Strand Annealing, Conservative Homologous Recombination, Nonhomologous DNA End Joining, and the Cell Cycle-Dependent Repair of DNA Double-Strand Breaks Induced by Sparsely or Densely Ionizing Radiation. *Radiation Research 171,* 265 – 273.

Glaab WE, Tindall KR, Skopek TR. 1999. Specificity of mutations induced by methyl methanesulfonate in mismatch repair-deficient human cancer cell lines. *Mutation Research 427*, 67 – 78.

Groth P, Ausländer S, Majumder MM, Schultz N, Johansson F, Petermann E, Helleday T. 2010. Methylated DNA Causes a Physical Block to Replication Forks Independently of Damage Signalling O^6-Methylguanine or DNA Single-Strand Breaks an Results in DNA Damage. *Journal of Molecular Biology 10*, 70 -82.

Gu J, Li S, Zhang X, Wang LC, Niewolik D, Schwarz K, Legerski RJ, Zandi E, Lieber MR. 2010. DNA-PKcs regulates single-stranded DNA endonuclease activity of Artemis. *DNA repair 9,* 429 – 437.

Gurley KE, Moser R, Gu Y, Hasty P, Kemp CJ. 2009. DNA-PK suppresses a p53-independent apoptotic response to DNA damage. *EMBO reports 10:1*, 87 – 93.

Hammel M, Yu Y, Fang S, Lees-Miller SP, Tainer JA. 2010 XLF regulats Filament Architecture of the XRCC4·Ligase IV Complex. *Structure 18*, 1431 – 1442.

Hiom K. 2010. Coping with DNA double strand breaks. *DNA repair 9,* 1256 – 1263.

Hu S, Cucinotta FA. 2011. Modelling the Way Ku Binds DNA. *Radiation Protection Dosimetry 143,* 169 – 201.

Iliakis G. 2009. Backup pathways of NHEJ in cells of higher eukaryotes: Cell cycle dependence. *Radiotherapy and Oncology 92, 310* – 315.

Jung HJ, Lee JH, Seo YR. 2009. Enhancement of Methyl Methanesulfonate-Induced Base Excision Repair in the Presence of Selenomethionine on p53-Dependent Pathway. *Journal of Medicinal Food 12:2*, 340 – 344.

Jaiswal AS and Narayan S. 2002. S_N2 DNA-alkylating agent-induced phosphorylation of p53 and activation of *p21* gene expression. *Mutation Research 500*, 17 – 30.

Karimi-Busheri F, Rasouli-Nia A, Allaluni-Turner et al. 2007. Human Polynucleotide Kinase Participates in Repair of DNA Double-Strand Breaks by Nonhomologous End Joining but not Homologous Recombination. *Cancer Research 67*, 6619 – 6625.

Karlsson KH and Stenerlöw B. 2007. Extensive ssDNA end formation at DNA double-strand breaks in non-homologous end-joining deficient cells during the S phase. *BMC Molecular Biology 26:8*, 97

Karlsson KH, Radulescu I, Rydberg B, Stenerlöw B. 2008. Repair of Radiation-Induced Heat-Labile Sites is Independent of DNA-PKcs, XRCC1 and PARP. *Radiation Research 169*, 506 – 512.

Kass EM and Jasin M. 2010. Collaboration and competition between DNA double-strand break repair pathways. *FEBS Letters 584,* 3703 – 3708.

Kriegs M, Kasten-Pisula U, Rieckmann T, Holst K, Saker J, Dham-Daphi J, Dikomey E. 2010. The epidermal growth factor receptor modulates DNA double-strand break repair by regulating non-homologous end-joining. *DNA repair 9,* 889 – 897.

Lamarche BJ, Orazio NI, Weitzman MD. 2010. The MRN complex in double-strand break repair and telomere maintenance. *FEBS Letters 584,* 3682 – 3695.

Lee MY, Kim MA, Kim HJ, Bae YS, Park JI, Kwak JY, Chung JH, Yun J. 2007. Alkylating agent methyl methanesulfonate (MMS) induces a wave of global protein hyperacetylation: Implications in cancer cell death. *Biochemical and Biophysical Research Communications 360*, 483 – 489.

Luke AM, Chastain PD, Pachkowski BF, Afonin V, Takeda S, Kaufman DG, Swenberg JA, Nakamura J. 2010. Accumulation of true single strand breaks and AP sites in base excision repair deficient cells. *Mutation Research 694*, 65 – 71.

Lundin C, North M, Erixon K, Walters K, Jenssen D, Goldman ASH, Helleday T. 2005. Methyl methanesulfonate (MMS) produces heat-labile DNA damage but no detectable *in vivo* DNA double-strand breaks. *Nucleic Acids Research 33:12*, 3799 – 3811.

Maas SA, Donghia NM, Tompkins K, Foreman O, Mills KD. 2010. Artemis stabilizes the genome and modulates proliferative response in multipotent mesenchymal cells. *BMC Biology 8*:132.

Mahaney BL, Meek K, Lees-Miller SP. 2009. Repair of ionizing radiation-induced DNA double-strand breaks by non-homologous end-joining. *Biochemical Journal 417*, 639 – 650.

Malivert L, Ropars V, Nunez M, Drevet P, Miron S, Faure G, Guerois R, Mornon JP, Revy P, Charbonnier JB, Cellebaut I, Villaray JP. 2010. Delineation of the Xrcc4-interacting Region in the Globular Head Domain of Cernunnos/XLF. *Journal of Biological Chemistry 285:30*, 26475 – 26483.

Mao Z, Bozzella M, Seluanov A, Gorbunova V. 2008. DNA repair by nonhomologous end joining and homologous recombination during cell cycle in human cells. *Cell Cycle 7:18,* 2902 – 2906.

Mazin VA, Mazina OM, Bugreev DV, Rossi MJ. 2010. Rad54, the motor of homologous recombination. *DNA repair 9,* 286 – 302.

Mishina Y, Duguid EM, He C. 2006. Direct Reversal of DNA Alkylation Damage. *Chemical Reviews 106:2*, 215 – 232.

Nemec AA, Wallace SS, Sweasy JB. 2010. Variant base excision repair proteins: Contributors to genomic instability. *Seminars in Cancer Biology 20*, 320 – 328.

Nagasawa H, Little JB, Lin YF, So S, Kurimasa A, Peng Y, Brogan JR, Chen DJ, Bedford JS, Chen BPC. 2011. *Radiation research 175,* 83 – 89.

Nikolova T, Ensminger M, Löbrich M, Kaina B. 2010. Homologous recombination protects mammalian cells from replication-associated DNA double-strand breaks arising in response to methyl methanesulfonate. *DNA repair 9*, 1050 – 1063.

Ochi T, Sibanda BL, Wu Q, Chirgadze DY, Bolanos-Garcia VM, Blundell TL. 2010. Structural Biology of DNA Repair: Spatial Organisation of the Multicomponent Complexes of Nonhomologous End Joining. *Journal of Nucleic Acids: 621 – 695*.

Park EJ, Chan DW, Park JH, Oettinger MA, Kown J. 2003. DNA-PK is activated by nucleosomes and phosphorylates H2AX within the nucleosomes in acetylation-dependent manner. *Nucleic Acids Research 31:23*, 6819 – 6827.

Rassool FV. 2003. DNA double strand breaks (DSB) and non-homologous end joining (NHEJ) pathways in human leukemia. *Cancer letters 193*, 1 – 9.

Ramadan K, Maga G, Shevelev IV, Villani G, Blanco L, Hübscher U. 2003. Huamn DNA Polymerase λ Possesses Terminal Deoxyribonucleotidyl Transferase Activity and Can Elongate RNA Primers: Implication for Novel Functions. *Journal of Molecular Biology 328,* 63 – 72.

Recuero-Checa MA, Dore AS, Arias-Palomo E, Rivera-Calzada A, Scheres SHW, Maman JD, Pearl LH, Llorca O. 2009. Electron microscopy of Xrcc4 and the DNA Ligase IV-Xrcc4 DNA repair complex. *DNA repair 8*, 1380 – 1389.

Robertson AB, Klungland A, Rognes T, Leiros I. 2009. Base excision repair: the long and short of it. *Cellular and Molecular Life Sciences 66*, 981 – 993.

Rydberg B. 2000. Radiation-Induced Heat-Labile Sites that Convert into DNA Double-Strand Breaks. *Radiation Research 153*, 805 – 812.

Stenerlöw B, Karlsson KH, Cooper B, Rydberg B. 2003. Measurement of Promt DNA Double-Strand Breaks in Mammalian Cells without Including Heat-Labile Sites: Results for Cell Deficient in Nonhomologous End Joining. *Radiation Research 159*, 502 – 510.

Taleei R, Weinfeld M, Nikjoo H. 2011. A kinetic model of single-stranded annealing for the repair of DNA double-strand breaks. *Radiation Protection Dosimetry 143,* 191 – 195.

Vispe S and Satoh MS. 2000. DNA repair patch-mediated double strand DNA break formation in human cells. *The Journal of Biological Chemistry 275,* 27386–27392.

Walker JR, Corpina RA, Goldberg J. 2001. Structure of the Ku heterodimer bound to DNA and its implications for double-strand break repair. *Nature 412,* 607 – 614.

Wang H, Perrault AR, Takeda Y, Qin W, Wang H, Iliakis G. 2003. Biochemical evidence for Ku-independent backup pathways of NHEJ. *Nucleic Acids Research 31,* 5377-5388.

West SC. 2003. Molecular views of recombination proteins and their control. *Nature Reviews Molecular Cell Biology 4,* 435 – 445.

Wilhelm D, Bender K, Knebel A, Angel P. 1997. The Level of Intracellular Glutathione Is a Key Regulator for the Induction of Stress-Activated Signal Transduction Pathways Including Jun N-Terminal Protein Kinases and p38 Kinase by Alkylating Agents. *Molecular and Cellular Biology 17*, 4792 – 4800.

Wilson III DM, Kim D, Berquist BR, Sigurdson AJ. 2010. Variation in base excision repair capacity. *Mutation Research*, in press.

Wyatt MD and Pittman DL. 2006. Methylating agents and DNA repair responses: methylated bases and sources of strand breaks. *Chemical Research Toxicology 19:12*, 1580 – 1594.